# Electron-Energy-Loss Spectra of Plasmonic Nanoparticles

Ulrich Hohenester,* Harald Ditlbacher, and Joachim R. Krenn

*Institut für Physik, Karl-Franzens-Universität Graz, Universitätsplatz 5, 8010 Graz, Austria*

(Received 21 January 2009; revised manuscript received 21 July 2009; published 31 August 2009)

We investigate electron-energy-loss spectroscopy (EELS) on metallic nanoparticles, through simulations, and provide a comprehensive comparison between EELS and the photonic local density of states (LDOS). Most importantly, we show that there is no direct link between EELS and LDOS maps, and that EELS can even be blind to *hot spots* in the gap between coupled nanoparticles. Although intimately related, the two quantities provide complementary information. This finding is in marked contrast to recently reported results.

DOI: 10.1103/PhysRevLett.103.106801 PACS numbers: 73.20.Mf, 78.20.Bh, 79.20.Uv

Electron-energy-loss spectroscopy (EELS) in combination with scanning transmission electron microscopy is emerging as a novel characterization tool in plasmonics [1–4]. The high spatial resolution of electron-based microscopy together with the improved energy resolution in the sub-eV range render EELS ideal for the study of plasmonics structures, with possible applications for optical data processing, negative refraction, or biosensors [5,6].

A drawback of the technique has so far been the lack of a consistent interpretation of experimental EELS data. Although the theoretical description of EELS on metallic nanoparticles is well established [7], it is less obvious how to interpret the results and, most importantly, how to relate them to the information extracted from optical experiments. As a first step in this direction, García de Abajo and Kociak [8] recently established a rigid relation between EELS and a generalized density of states. Using computer simulations, the authors speculated that this quantity might render directly the photonic local density of states (LDOS), which plays a crucial role for the optical properties of plasmonic nanoparticles [9].

In this Letter we reconsider EELS on flat metallic nanoparticles, such as those typically produced with electron beam lithography, and provide a comprehensive comparison between EELS and the photonic LDOS. Most importantly, we clearly demonstrate that there are marked differences between EELS and LDOS maps. We show that an electron beam couples differently to the surface plasmons than a dipole, and thus there exists no clear-cut relation between EELS and LDOS. For coupled nanoparticles, EELS turns out to be blind to the *hot spots* in the gap region between particles.

*Photonic local density of states.*—A dipole radiator, such as a molecule, provides a direct probe of the photonic LDOS [9]. When it is placed in the vicinity of a metallic nanoparticle, the modified dielectric environment enhances the radiative and nonradiative decay rates, which can be computed from the Fermi golden rule expression [10]

$$\frac{\hbar\Gamma_{\rm dip}}{2} = \mathrm{Im}[\boldsymbol{d}\cdot\boldsymbol{E}(\boldsymbol{r}_{\rm dip},\omega)]. \tag{1}$$

Here $\boldsymbol{d}$ is the dipole moment and $\boldsymbol{E}(\boldsymbol{r}_{\rm dip},\omega)$ is the electric field at the position $\boldsymbol{r}_{\rm dip}$ of the molecule and at the transition frequency $\omega$ (we use SI units throughout). Equation (1) describes a process reminiscent of a self-energy, where the dipole induces an electric field which acts back on the dipole itself. The real part of this coupling is associated with an energy renormalization, usually referred to as the *Lamb shift*, and the imaginary part accounts for the damping of the dipole excitation. We can use the dyadic Green function to relate the field to the dipole source viz.

$$\boldsymbol{E}(\boldsymbol{r},\omega) = \omega^2\mu_0\boldsymbol{G}(\boldsymbol{r},\boldsymbol{r}_{\rm dip},\omega)\cdot\boldsymbol{d}. \tag{2}$$

Upon insertion of this expression into Eq. (1), we obtain the relation [9]

$$\Gamma_{\rm dip} = \frac{2\omega}{3\hbar\epsilon_0}|\boldsymbol{d}|^2\rho_{\hat{\boldsymbol{n}}}(\boldsymbol{r}_{\rm dip},\omega) \tag{3}$$

between the dipole scattering rate $\Gamma_{\rm dip}$ and the photonic local density of states

$$\rho_{\hat{\boldsymbol{n}}}(\boldsymbol{r},\omega) = \frac{6\omega}{\pi c^2}\hat{\boldsymbol{n}}\cdot\mathrm{Im}\boldsymbol{G}(\boldsymbol{r},\boldsymbol{r},\omega)\cdot\hat{\boldsymbol{n}}. \tag{4}$$

Here $\hat{\boldsymbol{n}}$ is the unit vector pointing in the direction of the dipole. Usually one does not keep in $\rho_{\hat{\boldsymbol{n}}}(\boldsymbol{r},\omega)$ the direction dependence of the dipole, but averages over all direction angles instead [8]. The resulting expression then accounts for the local density of electromagnetic modes to which a dipole can couple. The higher the mode density, the faster the dipole will decay.

*Electron-energy-loss spectroscopy.*—An electron beam, where the electrons possess kinetic energies in the 100 keV range, provides an alternative probe for the dielectric environment of metallic nanoparticles. When passing by or through the nanoparticle, the electrons can excite surface plasmons and lose energy, which is subsequently monitored. By raster scanning the electron beam over the sample, one obtains a direct map of the electromagnetic environment. For sufficiently small particles we can employ the quasistatic approximation, where retardation effects due to the finite speed of light are neglected and only

 

the frequency dependence of the dielectric response function is considered.

The charge distribution of the electron beam propagating with velocity $v$ along $z$ is given by $\rho_{\text{ext}} = -e\delta(\boldsymbol{R} - \boldsymbol{R}_0)\delta(z - vt)$. Here, $e$ is the modulus of the electron charge, $\boldsymbol{R} = (x, y)$ and $z$ are, respectively, the position components perpendicular and parallel to the beam axis, and $\boldsymbol{R}_0 = (x_0, y_0)$ is the 2D impact parameter of the electron trajectory. Its Fourier transform in time

$$\rho_{\text{ext}}(\boldsymbol{r}, \omega) = -e\delta(\boldsymbol{R} - \boldsymbol{R}_0)\frac{e^{iz\omega/v}}{v} \tag{5}$$

corresponds to a charge distribution which oscillates along $z$. This form is due to the change of the reference frame underlying the Fourier transform. In the time domain, the electron beam interacts with a surface plasmon oscillating in time. In frequency space, the surface plasmon oscillation becomes frozen, and this frozen charge distribution now interacts with a periodically modulated $\rho_{\text{ext}}(\boldsymbol{r}, \omega)$ of the electron beam (with wave number $\omega/v$).

Again we encounter a process reminiscent of a self-energy, where the electron beam induces charge oscillations on the metallic nanoparticle, which produce an electromagnetic field that acts back on the electron beam. The induced potential can be computed by means of the electrostatic Green function [11]

$$\phi_{\text{ind}}(\boldsymbol{r}, t) = -\frac{e}{2\pi\epsilon_0 v}\int_{-\infty}^{\infty} d\omega dz' G_{\text{ind}}(\boldsymbol{r}, \boldsymbol{r}', \omega)e^{-i\omega(t - z'/v)}, \tag{6}$$

where $\boldsymbol{r}'$ has to be evaluated along the trajectory of the electron. Here $G_{\text{ind}}$ is that part of the Green function associated with the metallic nanoparticle only. The total energy loss is given by the work done against the field, which is induced by the excited surface plasmons. This results in a loss probability $\Gamma_{\text{EELS}}(\boldsymbol{R}_0, \omega)$ for an energy loss $\hbar\omega$ of the form [12]

$$\Gamma_{\text{EELS}}(\boldsymbol{R}_0, \omega) = \frac{1}{\pi\hbar\epsilon_0}\int_{-\infty}^{\infty} dz dz' \,\text{Im}[\rho^*_{\text{ext}}(\boldsymbol{r}, \omega) \times G_{\text{ind}}(\boldsymbol{r}, \boldsymbol{r}', \omega)\rho_{\text{ext}}(\boldsymbol{r}, \omega)]. \tag{7}$$

Thus, the energy loss probability is given by the average value of the imaginary part of the induced interaction.

Equation (7) relates the EELS rate to the Fourier transform of the Green function $G_{\text{ind}}(\boldsymbol{R}_0, \boldsymbol{R}_0, z, z', \omega)$. In a similar manner, one can relate $\Gamma_{\text{EELS}}$ to the Fourier transform of the $z$ component of the dyadic Green tensor, $G^{zz}_{\text{ind}}(\boldsymbol{R}_0, \boldsymbol{R}_0, z, z', \omega)$. This latter relation also holds for the solution of the full Maxwell equations, beyond the quasistatic limit, and is particularly useful for establishing a formal connection between EELS and LDOS [8].

*Eigenmode expansion.*—We next show that an electron beam interacts with the metallic nanoparticle in a distinctly different manner than a dipole. We consider the situation where the nanoparticle, described by a local and homogeneous dielectric function $\epsilon_m(\omega)$, is embedded in a background with dielectric constant $\epsilon_b$. The solution of the electrostatic problem is then provided by the free-space Green function $G(\boldsymbol{r}, \boldsymbol{r}') = 1/(4\pi|\boldsymbol{r} - \boldsymbol{r}'|)$ together with a surface charge $\sigma(\boldsymbol{s}, \omega)$ located at the boundary $\partial\Omega$ of the metallic nanoparticle. The potential is given by

$$\phi(\boldsymbol{r}, \omega) = \frac{1}{\epsilon_0}\int_{\partial\Omega} G(\boldsymbol{r}, \boldsymbol{s}')\sigma(\boldsymbol{s}', \omega)da' + \phi_{\text{ext}}(\boldsymbol{r}, \omega), \tag{8}$$

where the first and second term on the right-hand side account for the induced and external potential, respectively. The surface charge $\sigma$ is obtained from the requirement that the normal component of the dielectric displacement is continuous across the boundary. Introducing the surface derivative $F$ of the Green function, we get [13]

$$\Lambda(\omega)\sigma(\boldsymbol{s}, \omega) - \int_{\partial\Omega} F(\boldsymbol{s}, \boldsymbol{s}')\sigma(\boldsymbol{s}', \omega)da' = \epsilon_0\frac{\partial\phi_{\text{ext}}(\boldsymbol{s}, \omega)}{\partial\hat{n}}, \tag{9}$$

which allows us to compute the surface charge for the external excitation of a dipole or electron beam. The last term on the right-hand side denotes the surface derivative of $\phi_{\text{ext}}$, and $\Lambda(\omega) = \frac{1}{2}[\epsilon_m(\omega) - \epsilon_b]/[\epsilon_m(\omega) + \epsilon_b]$.

Equation (9) can be formally solved through the eigenvalues $\lambda_k$ and right eigenvectors $\sigma_k(\boldsymbol{s})$ of $F$, which, together with the left eigenvectors $\tilde{\sigma}_k(\boldsymbol{s})$, form a complete biorthogonal set [14]. Multiplying Eq. (9) from the left with $\tilde{\sigma}_k$ and integrating over the particle surface, we obtain

$$G_{\text{ind}}(\boldsymbol{r}, \boldsymbol{r}') = \sum_k \frac{\int G(\boldsymbol{r}, \boldsymbol{s})\sigma_k(\boldsymbol{s})da \int \tilde{\sigma}_k(\boldsymbol{s}')F(\boldsymbol{s}', \boldsymbol{r}')da'}{\Lambda(\omega) - \lambda_k} \tag{10}$$

for the induced potential at position $\boldsymbol{r}$, which originates from a unit charge located at position $\boldsymbol{r}'$. The integral with $\tilde{\sigma}_k$ describes how the surface plasmon mode $k$ is excited by the electric field of the unit charge, located at position $\boldsymbol{r}'$, and the integral with $\sigma_k$ accounts for the potential, at position $\boldsymbol{r}$, which in turn is induced by the plasmon. The plasmon resonances are associated with those frequencies $\omega$ where the denominator becomes small.

The EELS rate is obtained by inserting Eq. (10) into Eq. (7). Let us consider the case of flat nanoparticles, where the inverse of the wave number $q = \omega/v$ is much larger than the nanoparticle size. Indeed, for a typical kinetic electron energy of 100 keV and an energy $\hbar\omega = 1$ eV we obtain $\lambda = 2\pi/q \sim 700$ nm, which is significantly larger than typical nanoparticle dimensions of several tens of nanometers. The charge distribution of Eq. (5), through which the surface plasmons are excited, has therefore approximately the form of a charged wire, which is oriented along the direction $z$ of the electron beam. The resulting dependence of the potential on the lateral distance $\rho$ between electron beam and nanoparticle is of the form $\ln\rho$, rather than the usual $1/\rho$ dependence of a point

charge. For this reason, one readily appreciates that EELS probes the surface plasmon differently than a point charge. The same reasoning applies to a dipole probe, which measures the photonic LDOS and has a $1/\rho^2$ distance dependence. Thus, the relation between EELS and LDOS is at best qualitative, but there is no direct link between the two quantities.

*Simulation results.*—To investigate the qualitative correspondence between EELS and LDOS, we additionally performed simulations using the boundary element method approach [10,13]. Figure 1(a) shows a simulated EELS map for an elongated, disk-shaped metallic nanoparticle, together with the LDOS, the LDOS projected along $z$, $\rho_z$, and the potential given by the imaginary part of $G_{\mathrm{ind}}(\boldsymbol{R}, \boldsymbol{R}, z, z, \omega)$. All quantities are computed in the symmetry plane of the particle and at the photon energy of the dipole plasmon mode. Apparently, neither the angle-averaged LDOS nor the LDOS projected along $z$ resemble the EELS map. The only similarity is between EELS and potential. When we move away from the particle, Fig. 1(b), we find that the EELS map is similar to the potential and LDOS in planes 20 and 40 nm above the particle. Similar conclusions hold for the quadrupole plasmon mode shown in Figs. 1(c) and 1(d).

In Fig. 2 we investigate the case of two coupled nanoparticles. The surface plasmons of lowest energy correspond to bonding and antibonding modes, where the dipole moments of the two particles are oriented, respectively, parallel and antiparallel to each other. Again, EELS and LDOS strongly differ in the symmetry plane of the nanoparticles. This is seen most strikingly at the "hot spot" in between the two particles. For the bonding mode in 2(a), the LDOS is very high in the region between the two particles. This is due to the strong fields in the gap region associated with the bonding surface plasmon mode. In contrast, EELS is completely blind to the hot spot. The situation is reversed for the antibonding mode. Here, the LDOS drops at the center point, due to the vanishing field of the antibonding plasmon mode (note that the dipole still couples to other modes, thus keeping the LDOS finite), whereas the EELS rate has a pronounced maximum in between the two particles. Once again we find that the projected LDOS and potential qualitatively resemble the EELS maps in a plane above the nanoparticle, as shown in the lower panels of Fig. 2.

*Discussion.*—Why do EELS and LDOS differ so strongly in the vicinity of the nanoparticle? To understand this, in the following we analyze the EELS rate in more detail. We replace the upper and lower integration limits in the double integral of Eq. (7) by some cutoff value $z$, and plot in Fig. 3(a) the *incremental EELS rate* $\partial\Gamma_{\mathrm{EELS}}(\boldsymbol{R}_0, \omega; z)/\partial z$ (averaged over all beam positions $\boldsymbol{R}_0$), which provides a measure of large integrand regions. One observes that the maximum of the integrand is approximately 20 nm above the nanoparticle. A similar analysis can be made for the relation between EELS and LDOS, by replacing in Eq. (7) the Green function $G_{\mathrm{ind}}$ with the dyadic Green function $G^{zz}_{\mathrm{ind}}$ [8]. Figure 3(a) shows that in this case the maximum of the integrand is shifted to a distance of about 50 nm. This is a counterintuitive result, as one would expect that a dipole (corresponding to $G^{zz}_{\mathrm{ind}}$)

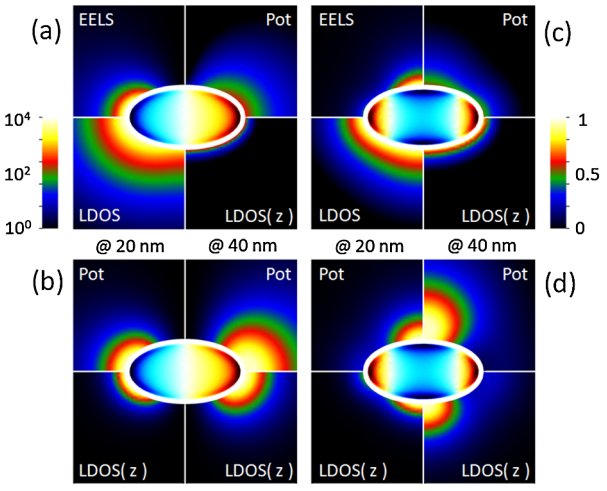


FIG. 1 (color online). EELS, LDOS, and potential maps for a metallic nanoparticle with a long axis of 70 nm, an axes ratio of 6:3:1, and at 1.6 and 2.1 eV photon energies corresponding to the surface plasmon modes of lowest energy. (a) EELS, LDOS, and potential at the photon energy of the dipolar plasmon mode, computed in the symmetry plane of the nanoparticle, and (b) 20 and 40 nm above. (c),(d) Same as (a),(b) but at the energy of the quadrupole plasmon mode. On the surface of the metallic nanoparticle, we show the surface charge distribution of the corresponding surface plasmon modes. In (a) and (c) we plot the potential and LDOS (in units of its free-space value) in a logarithmic scale and use a linear scale normalized to the maximum value otherwise. In all simulations we use for $\epsilon_m(\omega)$ a gold dielectric function [16] and set $\epsilon_b = 2.25$. The electron beam is assumed to have a kinetic energy of 100 keV.

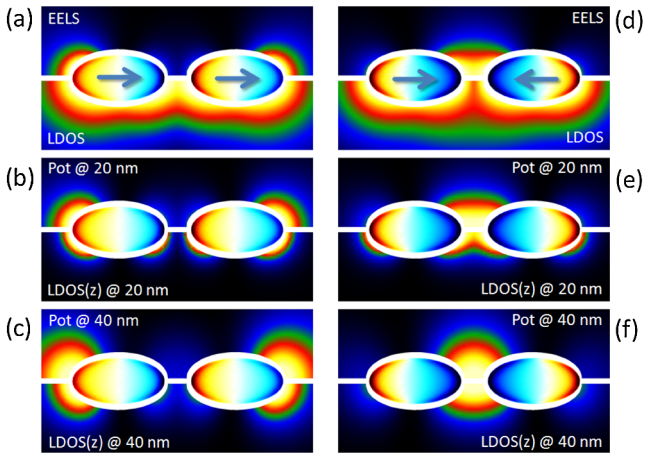


FIG. 2 (color online). Same as Fig. 1 but for coupled nanoparticles, and for (a)–(c) bonding surface plasmon mode (1.57 eV) and (d)–(f) antibonding mode (1.66 eV). Panels (a) and (d) show EELS and LDOS in the symmetry plane of the particle. The other panels report results for the potential and the projected LDOS in planes 20 and 40 nm above the particles.

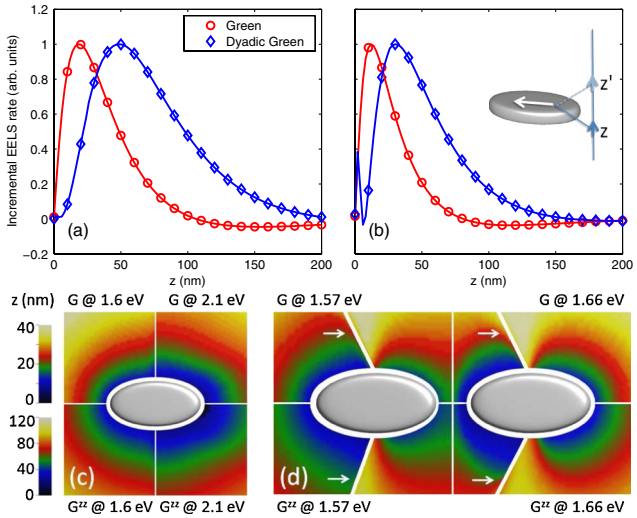


FIG. 3 (color online). Incremental EELS rate, as defined in text, for single nanoparticle depicted in Fig. 1 and at (a) dipole and (b) quadrupole surface plasmon energy. (c),(d) $z$ value where incremental EELS rate is maximal for electrostatic ($G$) and dyadic ($G^{zz}$) Green function. For the coupled particles (d), we do not show the results for points with too small EELS rates (indicated with arrows).

couples more strongly to the surface plasmons *closer* to the nanoparticle than a point charge (corresponding to $G_{\mathrm{ind}}$).

The reason why the integrand with the dyadic Green function $G^{zz}_{\mathrm{ind}}$ does not contribute for small $z$ values is due to interference. Recall that the dyadic Green function describes a process where a dipole at position $z$ induces a surface plasmon that acts back on a dipole at position $z'$, as schematically shown in the inset of 3(b). The surface plasmon is induced such that the resulting electric field causes an energy loss of the oscillating dipole, corresponding to a positive LDOS. In contrast, a dipole at the mirror position $-z$ will gain energy because it is driven with opposite phase. When performing an integration along $z$, as in the expression for the generalized LDOS, there will be an almost complete cancellation of these interactions with opposite signs. The magnitude of $\rho_z(\boldsymbol{R}, q, \omega)$ is thus determined by the asymptotic regions rather than those with a high LDOS. This explains why the LDOS close to the nanoparticle is totally unrelated to the EELS map. As no corresponding cancellation occurs in the case of the electrostatic Green function $G_{\mathrm{ind}}$, due to the underlying monopole-type coupling, the correspondence between EELS and potential appears to be the more natural one.

We also found that for $\partial\Gamma_{\mathrm{EELS}}(\boldsymbol{R}_0, \omega; z)/\partial z$ the maxima are at smaller $z$ values when $\boldsymbol{R}_0$ is located closer to the nanoparticle, as shown in Figs. 3(c) and 3(d). This is because close to the particle the electron beam interacts with the evanescent fields of the surface plasmons, and the interaction is bound to a small $z$ region, whereas farther away the beam interacts over a longer distance with the more extended field components. For this reason, there exists no "optimal" distance for the calculation of the potential or LDOS maps. Indeed, we found that any quantitative comparison between EELS and LDOS maps is doomed to failure [15].

In conclusion, we have investigated the relation between LDOS and EELS for flat metallic nanoparticles. We have shown that an electron beam and a dipole couple differently to the surface plasmons, and there exists no direct quantitative connection between EELS and LDOS, although the qualitative agreement is often fairly good. EELS has been shown to be blind to hot spots in the gap region between coupled nanoparticles. Electron-energy-loss spectroscopy is expected to become a highly powerful tool for the characterization of plasmonic devices, but care has to be taken in the proper interpretation of the experimental data.

*http://nanooptics.uni-graz.at

[1] N. Yamamoto, K. Araya, and F. J. García de Abajo, Phys. Rev. B **64**, 205419 (2001).
[2] J. Nelayah, M. Kociak, O. Stephan, F. J. Garcia de Abajo, M. Tence, L. Henrard, D. Taverna, I. Pastoriza-Santos, L. M. Liz-Martin, and C. Colliex, Nature Phys. **3**, 348 (2007).
[3] B. Schaffer, U. Hohenester, A. Trügler, and F. Hofer, Phys. Rev. B **79**, 041401(R) (2009).
[4] J. Nelayah, L. Gu, W. Sigle, C. T. Koch, I. Pastoriza-Santos, L. M. Liz-Martin, and P. A. van Anken, Opt. Lett. **34**, 1003 (2009).
[5] E. Orzbay, Science **311**, 189 (2006).
[6] H. Atwater, Sci. Am. **296**, No. 4, 56 (2007).
[7] A. Rivacoba, N. Zabala, and J. Aizpurua, Prog. Surf. Sci. **65**, 1 (2000).
[8] F. J. Garcia de Abajo and M. Kociak, Phys. Rev. Lett. **100**, 106804 (2008).
[9] L. Novotny and B. Hecht, *Principles of Nano-Optics* (Cambridge University Press, Cambridge, England, 2006).
[10] U. Hohenester and A. Trügler, IEEE J. Sel. Top. Quantum Electron. **14**, 1430 (2008).
[11] J. D. Jackson, *Classical Electrodynamics* (Wiley, New York, 1999).
[12] N. Zabala and A. Rivacoba, Phys. Rev. B **48**, 14 534 (1993).
[13] F. J. Garcia de Abajo and A. Howie, Phys. Rev. B **65**, 115418 (2002).
[14] I. D. Mayergoyz, D. R. Fredkin, and Z. Zhang, Phys. Rev. B **72**, 155412 (2005).
[15] Our results would not be significantly modified if retardation effects were considered, in agreement with the conclusions of Ref. [7]. Additional calculations (not shown) based on the full Maxwell equations revealed very similar results, with the main difference that the plasmon resonances are shifted slightly to the red.
[16] P. B. Johnson and R. W. Christy, Phys. Rev. B **6**, 4370 (1972).